Title: Cd(II) capture ability of an immobilized, fluorescent hexapeptide

Gábor Galbács,[1] Hajnalka Szokolai,[1] Attila Kormányos,[1] Anikó Metzinger,[1] Levente Szekeres,[1] Claudiu Marcu,[2] Francisc Peter,[2] Cornelia Muntean,[3] Adina Negrea,[3] Mihaela Ciopec,[3] and Attila Jancsó[*1]

[1]Department of Inorganic and Analytical Chemistry, University of Szeged, 6720, Szeged, Dóm tér 7, Hungary

[2]Faculty of Industrial Chemistry and Environmental Engineering, Politehnica University of Timișoara, Victoriei Sq. 2, 300006, Timișoara, Romania

[3]Faculty of Industrial Chemistry and Environmental Engineering, Politehnica University of Timișoara, 6 Bv. V. Parvan, 300223, Timișoara, Romania

Received: September 28, 2015; E-mail: jancso@chem.u-szeged.hu

Synopsis: A novel, cysteine-containing fluorescent hexapeptide, *N*-acetyl-Tyr-Cys-Ser-Ser-Cys-Tyr– (YY), targeting Cd(II) ion sensing, was synthesized on various solid supports including two resins, as well as glass and quartz surfaces. The synthesis was based on the Fmoc (9-fluorenylmethoxycarbonyl) and the APTES (3-aminopropyltriethoxysilane) methodologies on the resin and silica supports, respectively. The immobilized ligand, except when coupled to a hydrophobic benzhydrylamine resin, showed a remarkably efficient, pH-dependent Cd(II) capturing ability with a maximum binding capacity around neutral pH. The effect of contact time and metal ion concentration was also studied with a hydrophilic resin supported peptide (YY-NTG). The interaction of YY-NTG with Cd(II) was investigated by pH-potentiometric titrations in aqueous samples containing the resin beads and Cd(II). These studies, together with metal ion capturing experiments under buffer-controlled pH, prove that

each immobilized peptide can bind one Cd(II) ion at pH=7.0 in the presence of one equivalent metal ion or metal ion excess. For Cd(II) binding to YY-NTG a notably high, K=1.3×10^{10} apparent stability constant was determined (1:1 metal-to-ligand ratio, pH=7.0). Analytical results suggests that the concentration of Cd(II) can be measured below 200 nM with this silica-supported peptide. The usefulness of the probe was demonstrated by fluorescence spectroscopy.

Keywords: immobilized synthetic oligopeptide, fluorescent quenching, molecular probe, cadmium(II) ion sensing

Introduction

The detection of toxic metal ions (e.g. heavy metals) in aqueous environmental and medical matrices has always been targeted by intense research. Well-established, routine spectroanalytical methods (e.g. ICP-AES, ICP-MS, GFAAS, etc.) are available to carry out such analyses, but optochemical sensors have also been suggested to be used for this purpose, by e.g. covalently attaching a suitable molecular probe to the surface of an optical fiber (e.g. lumogallion was used for the measurement of Al(III),[1] dihydroxyisoamethryin for uranyl,[2] dithizone for Pb(II) [3] etc.). The advantages of optochemical sensors in this application include the possibility for in-situ/on-site or even remote, and fast trace analyses with low cost and very low sample requirements. A particularly interesting and promising research direction in this area is the utilization of bio-inspired receptors - thus making them a sub-group of biosensors. Proteins, oligopeptide sequences [4] or even simple cells all have selective metal binding characteristics that make them promising biochemical metal-ion receptors. Several studies already reported about the successful use of such receptors in optochemical sensors;

these were reviewed by Imperiali et. al. in 1999,[5] Prodi et. al. in 2000,[6] Verma and Singh in 2005 [7] and very recently by Liu et. al..[8] The cell-based metal-ion biosensors are relatively cheap to produce, but often exhibit a slow response, obtaining a concentration-related signal from them is problematic and their use is limited to the conditions under which the given cells can live.[7–9] As opposed to this, synthetic oligopeptide sensors are somewhat costlier, but can be made very selective and sensitive, and their operating conditions are less limited. Fluorophore labeled oligopeptides have been shown to be capable for the detection of transition metal ions via fluorescence signaling based on turn-off [10,11] turn-on [12–14] or intramolecular energy transfer based mechanisms.[15,16] The design of the described peptides were inspired by e.g. zinc(II)-binding motifs of zinc-finger proteins [15,17] typical metal-binding sequences of various metalloproteins [10,16,18,19] or were rationally designed by the combination of metal-binding amino acids.[11–14,20,21] Nevertheless, there have been very few attempts for the characterization of such sequences in immobilized forms [10,22] that would be essential from the point of view of sensor development.

To date, only a few fluorescent probes have been described in the literature for the sensing of Cd(II) ions; a recent review by Dutta and Das [23] on toxic metal ion selective fluorescent sensors lists nine different Cd(II) probes. The developed fluorescent probes were mainly based on crown ether- [24,25] and anthracene-based [26,27] structures, but proprietary aromatic structures, including dipyridyl-phenantroline,[28] as well as naphthyridine-based [29] and tricarbocyanine-based molecules [30] were also described. There are only a very few examples for fluorescent Cd(II)-sensing synthetic peptides [18,31,32] but none of these probes were immobilized on a solid support. Limit of detection (LOD) values are scarcely reported in the literature for the Cd(II) fluorescent probes, most probably due to the fact that LODs would be not only influenced by the probe but also largely by the sensor construction itself. The

published values range from nM to μM [18,23,32] (for two reported peptidyl probes: 41 nM [18] and 294 nM [32]).

The metal-ion binding features of several short oligopeptides, containing two cysteine residues, have already been investigated in our group from different perspectives.[33,34] The studied 12-mer oligopeptide ligands proved to coordinate the studied group-12 metal ions (Zn(II), Cd(II) and Hg(II)) rather efficiently. Reports discussing the heavy metal ion binding capabilities of similar compounds, such as cysteine and poly-L-cysteine,[35,36] as well as poly-L-aspartate,[37] coupled to various solid supports (e.g. controlled-pore glass or a porous carbon surface) can also be found in the chemical literature.

In the present paper, we report on the synthesis and characterization of the Cd(II) binding properties of a novel, cysteine and tyrosine-containing hexapeptide receptor molecule (probe), immobilized on several solid supports and designed for potential future use in "turn-off" type fluorescent optochemical sensors.

Experimental

Chemicals and materials

Metal ion stock solutions for the Cd(II)-binding experiments were prepared from $CdCl_2 \times xH_2O$ (Aldrich). A solution containing a mixture of Cd(II), Zn(II), Ni(II) and Pb(II) ions were prepared from $Cd(NO_3)_2 \times 4H_2O$ (Alfa Aesar), $Zn(NO_3)_2 \times 6H_2O$ (Fluka), $Ni(NO_3)_2 \times 6H_2O$ (Sigma-Aldrich) and $Pb(NO_3)_2$ (Sigma-Aldrich). The concentration of all metal-ion stock solutions were determined by inductively coupled plasma mass spectrometry (see later). pH-metric titrations were performed using a NaOH (Aldrich) standard solution.

The chemicals and reagents used in the experiments, such as the protected *N*-α-Fmoc-O-tert-butyl-L-tyrosine, *N*-α-Fmoc-S-trityl-L-cysteine and *N*-α-Fmoc-O-tert-butyl-L-serine amino acids, 2-(1H-benzotriazole-1-yl)-1,1,3,3-tetramethyluronium hexafluorophosphate (HBTU), N-hydroxybenzotriazole (HOBt), benzhydrylamine resin (BHA-resin·HCl), Novasyn TG amino resin (all from Novabiochem), *N*,*N*-diisopropylethylamine (DIPEA), diethylether (both from Sigma), triisopropylsilane (TIS), 1,2-ethanedithiol (EDT), piperidine (all from Aldrich), pyridine (Merck), acetic anhydride (Fluka), trifluoroacetic acid (TFA), trifluoromethanesulfonic acid (TFMSA), thioanisole (TA), phenol (all from Sigma-Aldrich), 1-methyl-2-pyrrolidone (NMP), dichloromethane, methanol (all from Molar Chemicals), acetonitrile (BDH Prolabo Chemicals), and 3-aminopropyltriethoxysilane (APTES) (Alfa Aesar) were all of analytical purity and were used without any further purification. Cleaning of glassware and silica supports were carried out using a mixture of Suprapur trace analytical purity cc. H_2SO_4 and 30 v/v% H_2O_2 (both from Merck) and thorough rinsing by deionized water from a Millipore Elix 5 + Synergy labwater system. Quartz microscope slides were purchased from Ted Pella, whereas glass slides from Menzel-Gläser were used. Calibration stock solutions and internal standard solution used in atomic mass spectrometry experiments were obtained from Agilent and Inorganic Ventures.

Peptide synthesis on synthetic resins

The hexapeptide *N*-acetyl-Tyr-Cys-Ser-Ser-Cys-Tyr– (referred to as "Ac-YCSSCY–" or simply by "YY–" further on) was synthesized on co-polymer resin beads by solid phase peptide synthesis using Fmoc methodology (Fmoc = 9-fluorenylmethoxycarbonyl). Two resins with different swelling properties were selected for use in the experiments after considering the need of performing side-chain de-protection without breaking the bonds

linking the peptide to the solid supports. The benzhydrylamine resin (BHA-resin·HCl, 100-200 mesh, loading: 0.77 mmole/g) with a co-poly(styrene-divinylbenzene) (1% DVB) matrix has a poor swelling character in water, nevertheless, the benzhydrylamine linker allows the cleavage of the peptide by TFMSA and thus the verification of the success of synthesis. The other investigated support, an aminomethyl functionalized resin (Novasyn TG amino resin, 90 μm, 0.26 mmole/g), swells very well in aqueous media owing to the polyethylene glycol polystyrene composite matrix, however, the acid-stability of the peptide-linkage does not allow the cleavage of the intact peptide for testing purposes. The two different resin-supported hexapeptides will be denoted in the following sections as YY-BHA and YY-NTG.

The amino acid building blocks were applied in a four-fold excess compared to the given loading values of the resins and double-coupled in each step of the synthesis by applying HBTU (4.0 eq./building block), HOBt (4 eq./building block) and DIPEA (8.0 eq./building block). The coupling reactions (t = 1 h) were performed in NMP. The Fmoc-protecting groups were removed by using a solution of 20% v/v piperidine in NMP (t = 3 min, repeated 4 times). The success of the attachment of the amino acid residues were monitored by the Kaiser-test.[38] In the case of successful couplings, the potentially remaining small fraction of unreacted amino nitrogens were acetylated with a mixture of acetic anhydride, DIPEA and dichloromethane (10–10–80% v/v) to minimize the possibility of the formation of any deleted peptide sequences (t = 15 min, repeated 2 times). The last coupling step was followed by the removal of the Fmoc protection from the terminal amino group of the Tyr-residue which was acetylated afterwards. Before further synthetic steps, the resin was rinsed by dichloromethane and methanol and dried in vacuum. Side-chain protecting groups were removed by a mixture of TFA, H_2O, EDT, phenol and TIS (92–2.5–2.5–2–1 % v/v) (t = 2 h) and the resin was washed by TFA, methanol, dichloromethane and finally by methanol and

dried in vacuum overnight. Both of the synthesized products were stored at 4 °C, in argon atmosphere.

The composition the final peptide synthesized on the BHA-resin was verified by cleaving the peptide off from the solid support in a form of peptide carboxamide. 100 mg of the peptide-decorated resin was stirred in a mixture of TA, EDT, TFMSA and TFA (8–4–8–80 % v/v) for 1.5 h at room temperature. Before adding TFA and then TFMSA, the resin was pre-cooled at −5…−10 °C on salted ice and stirred for 0.5 h in the presence of TA and EDT. The peptide was precipitated in cold diethyl ether and centrifuged for 15 min at 4000 rpm. The liquid phase was then removed and the crude product was dissolved in water and lyophilized to dryness. The obtained peptide was identified by ESI-MS.

For the purposes of fluorescence experiments, the hexapeptide YY, with a carboxamide group at the C-terminus, was also prepared on a Rinka Amide AM resin (Novabiochem, 200-400 mesh, loading: 0.68 mmol/g) which allowed the cleaving of the peptide from the resin. The synthesis protocol, up to the last step, was identical to that described above, however, the handling of the resin with the mixture of TFA, H_2O, EDT, phenol and TIS (see the composition above) for 3 h lead to a cleaving of the peptide off the beads in parallel with the removal of the amino acid sidechain protecting groups. The peptide was then precipitated in cold diethyl ether, dissolved in water and purified by RP-HPLC using a Supelco Discovery BIO Wide Pore C18 (25×10 mm, 5 μm) semi preparative column. The mixtures of water and acetonitrile containing 0.05% TFA (Eluent A: H_2O-CH_3CN 95:5 %v/v with 0.05% TFA, Eluent B: H_2O-CH_3CN 5:95 %v/v with 0.05% TFA) were used for the elution of the peptide, applying the following elution program:
0-28 min: 12% B (isocratic); 28-31 min: 12-20% B (linear gradient); 31-35 min: 20% B (isocratic); 35-36 min: 20-12% B (linear gradient); 36-42 min: 12% B (isocratic).

The purity of the collected YY ligand was checked by HPLC (R_t = 24.2 min) and the peptide was identified by ESI-MS (see in the "Instrumental").

In order to obtain a reference material for the metal ion binding studies, a batch of the Novasyn TG amino resin was reacted with a mixture of acetic anhydride, DIPEA and dichloromethane (10–10–80% v/v). The aim of the acetylation of the terminal aminoalkyl functions was to prevent the Cd(II)-binding of the originally free primary amino groups. Please note, that the potentially unreacted amino groups of the peptide loaded Novasyn TG amino resin were also acetylated. This material will be referenced as capped-NTG throughout the text.

Peptide synthesis on silica surfaces

The peptide immobilization method developed was based on the procedures described by Carré [39] and M. Phaner-Goutorbe.[40] The method involves a cleaning step and two synthesis steps. In the cleaning step, the surface of the silica supports (conventional glass or quartz slides cut to 15 x 25 x 1 mm size) was cleaned using an oxidizing, highly acidic solution (3:1 ratio of cc. H_2SO_4 and 30% v/v H_2O_2) followed by sonication, and washing with deionized water as well as ethanol. The cleaning was completed by drying the silica supports under an infrared lamp.

The silanization was carried out in a 10% v/v aqueous APTES solution. The contact time was 30 min, after which all supports were rinsed and dried. In the last step of the immobilization, the actual in-situ peptide synthesis, based on a modified Fmoc-methodology [41], was carried out by attaching the first amino acid block to the free amino group of APTES and then continuing the synthesis block-by-block. Accurate loadings for the synthesis could not be calculated, due to the (relative) roughness and variations in the density of the hydroxyl

groups of the silica surfaces. Hence, we employed a large excess (ca. ten-fold) of the building blocks and coupling reagents based on the ca. 2.5 per nm^2 estimated density of hydroxil groups present on silica surfaces (which is equivalent to a total of ca. $1.875 \cdot 10^{15}$ binding sites, or $3.125 \cdot 10^{-9}$ mol, on both sides of the plates) and assuming a complete silanization. Each coupling was repeated twice (2+1 h). We did not perform the acetylation reaction after each coupling, only after adding the last amino acid. After the completion of the synthesis, the peptide chain was not cleaved from the surface, only the side-chain protecting groups were removed. The slides with the immobilized peptides were then rinsed with methanol, dried, and then stored under argon at 4 °C until further use. For easy referencing, the immobilized peptide on the glass and quartz surface will be abbreviated as YY-G and YY-Q.

The silanization and peptide synthesis were both carried out in a PTFE/PP reactor (Figure S1 in the Supporting Information) specially designed and fabricated for these procedures. In the reactor, five silica plates, each of them measuring 15 x 25 x 1 mm, could be processed in parallel, employing approximately 8 mL reagents and shaking on a horizontal shaker.

The silanization by APTES is a very important step in the immobilization procedure, as it is responsible for creating all binding sites for the peptide synthesis. Thus, the surface coverage, which in turn determines the overall analytical signal obtainable from the sensor transduction mechanism, largely depends on the success and efficiency of the silanization step. In spite of its importance, the success and quality of silanization by APTES or other functionalized silanes is rarely tested in the literature. In the present study, we performed various of such tests for both types of silica supports to characterize the treated surfaces; namely, we did SEM, FT-IR and AFM measurements and carried out the nanoparticle adsorption test.[39] These tests proved the success of silanization. We hereby present the results for the AFM and nanoparticle adsorption method. Figure 1 shows AFM scans taken before

and after silanization from both types of supports on 1 μm^2 areas in tapping mode. As it can be seen, the nature of the surface slightly changed due to the silanization; the number of the nanometer-scale surface corrugations largely increased. The APTES-silanized regions are identified as protruding, small, light coloured spots in the images, which cover the scanned areas evenly.[42]

The nanoparticle adsorption test detects the presence of free amino groups on the substrate's surface formed as a result of the successful APTES binding. If an APTES-treated silica slide is brought in contact with gold nanoparticles, the nanoparticles electrostatically attach themselves to the free amino groups, thereby staining the silica slide darker. In our experiments, the slides were immersed for 18 h in a nanosol containing 10 nm gold nanoparticles in 0.02 mM concentration. After rinsing the slides with deionized labwater and drying, the staining was apparent for the naked eye, and could also be detected by UV-Vis spectrophotometry (Figure 2). The gold nanoparticles did not stain the untreated silica.

Instrumental

Structural verification of the synthesized hexapeptide was performed by mass spectrometry, using a TSQ-7000 triple quadrupole mass spectrometer (Finnigan-MAT) equipped with an electrospray ionization (ESI) source. The instrument was operated in positive ion mode, with the ESI needle voltage set at 4.5 kV and using N_2 as carrier gas. Analytical data for Ac-YCSSCY-NH_2: m/z = 766.3 $[M+H]^+$, whereas the calculated monoisotopic molecular mass is 765.25.

In all experiments that required the determination of metal ion concentrations, an Agilent 7700x ICP-MS instrument was used, in the helium mode of the OSR^3 collisional cell and ^{103}Rh as internal standard. Multi-point calibration was performed using solutions prepared

from a certified stock standard solution (Inorganic Ventures) and trace quality deionized lab-water (Millipore Elix Advantage 5 + Synergy). The ^{111}Cd mass peak was used for quantitation. All labware was prepared for use by cleaning with ultratrace grade nitric and hydrochloric acids (Suprapur, Merck) followed by a thorough rinsing by the above labwater and dried under a laminar flow clean bench (AuroScience).

Fluorimetric studies were performed on a Hitachi-F4500 spectrofluorimeter using a 1.0 cm × 1.0 cm quartz cell equipped with a Teflon stopper. Emission spectra were recorded in the wavelength range of 285 – 400 nm with excitation at 278 nm, applying 5 nm and 10 nm slit widths for the exciting and emitted beams, respectively. The experiments were performed at pH = 7.0 (t = 25 °C) and with a varying Cd(II)-concentration ($c_{Cd(II)}$ = 1.25 – 30 μM) whereas the concentration of the peptide was kept constant at c_{YY} = 10 μM. After elimination of the background, the spectra were corrected for the inner filter effects according to the equation:[43]

$$F_{corr} = F_{obs} \times 10^{(A_{ex}+A_{em})/2}$$

where F_{corr} and F_{obs} are the corrected and observed fluorescence intensities, while A_{ex} and A_{em} stand for the observed absorbances of the samples at the excitation and emission wavelengths, respectively.

Protonation and Cd(II)-binding processes of YY-NTG were followed by potentiometric pH titration in aqueous mixtures (I = 0.1 M $NaClO_4$, T = 298.0 ± 0.1 K) containing ca. 0.03 g of the resin both in the Cd(II)-containing and Cd(II)-free samples. An automatic titration set including a PC controlled Dosimat 665 (Metrohm) autoburette and an Orion 710A precision digital pH-meter equipped with a Metrohm Micro pH glass electrode was used during these experiments. A continuous argon flow through the titration cell prevented the samples from contact with ambient air, which could have resulted in an oxidation of the peptide. Accurate conversion of the relative electrode potential values to

hydrogen ion concentrations was done by a method described in one of our earlier publications.[34] The protonation and complex formation equilibria of the immobilized ligand were characterized by the following general equilibrium process:

$$pM + qH + rL \rightleftharpoons M_pH_qL_r$$

$$\beta_{M_pH_qL_r} = \frac{[M_pH_qL_r]}{[M]^p[H]^q[L]^r}$$

where M denotes the metal ion, L the non-protonated immobilized YY ligand, and H the protons. Charges are omitted for simplicity, but can be easily calculated taking into account the composition of the fully protonated hexapeptide (H_4L). Formation constants for the protonation and metal ion binding processes and according to the above equations were calculated by the computer program PSEQUAD.[44] Protonation constants were determined from two independent titrations (60-80 data points per titration). Several titrations were carried out with different Cd(II):immobilized YY ratios (i.e. 0.5:1, 1:1 and 2:1) calculated on the basis of the theoretical loading of the resin and the applied quantity of YY-NTG (ca. 30 mg for each titration). The applicability of the theoretical peptide content of the resin was confirmed by the evaluation of potentiometric titrations and also indirectly by a metal-capturing experiment performed in a solution buffered to pH = 7.0 (see the chapter "Effect of pH buffering" later in the text). The deviation of the logβ values for the protonation processes of YY-NTG determined from the parallel experiments was around 0.1 log unit which is a reasonable uncertainty for such an immobilized system and shows a good reproducibility of the data. Each titration curve contained 60-80 data points. In the presence of metal ion excess, precipitate formation could be observed above pH ~ 8 which was also reflected by the shape of the titration curves, and thus pH-potentiometric data of samples with metal ion excess were not evaluated. Owing to the slower equilibration as compared to titrations in homogenous aqueous solutions, waiting times between the dosing steps of base addition steps were allowed

to change according to the need for pH-stabilization which resulted in 3 – 4 h titration time. Neither the shape of the titration curves, nor the determined formation constants showed any sign of polyelectrolyte effect, that is the immobilized ligands could be handled as independent molecules (similarly to a homogenous solution). Nevertheless, owing to processes occurring on a solid-liquid interface and the technical difficulties of performing the titration in solutions containing resin beads, the accuracy of the results was somewhat poorer than that achievable with homogeneous aqueous samples and the obtained data should be considered as good estimates only.

Testing of the success of the silanization of silica substrates was performed using a PSIA XE100 type atomic force microscope (AFM) in tapping mode. The investigated area varied between 0.5-5 μm^2. The presence of free amino groups (APTES) on the surface of the supports was tested by FT-IR measurements and the nanoparticle adsorption method. The UV-Vis spectra of untreated and gold nanosol-treated silica surfaces were recorded using a Thermo Scientific Evolution 220 spectrometer, in the range between 400-800 nm. FT-IR measurements were performed using a Bio-Rad Digilab Division FTS-65A/896 Fourier transform infrared spectrometer equipped with a Harrick's Meridian® SplitPea single-reflection diamond attenuated total reflectance (ATR) accessory. All infrared spectra were recorded between 400 and 4000 cm^{-1}, at 4 cm^{-1} optical resolution and by averaging 256 interferograms.

Sample preparation for metal capturing studies

The Cd(II)-binding properties of the immobilized synthetic hexapeptide probe was investigated on all supports (resin beads and silica plates). For the purposes of these studies, all samples were prepared according to the concept described in this section for the resin-

based samples. 10.0 mg (±1 %) of the selected resin-supported peptide was added to a glass vessel containing 10.00 mL of a $CdCl_2$ solution, whose pH was pre-adjusted by strong bases/acids (NaOH/$HClO_4$ solutions) to the desired value and carefully degassed by argon to prevent the potential oxidation of the cysteine residues of the peptide. Concentration of the $CdCl_2$ solution was varied in the range of 6.2×10^{-5} – 7.1×10^{-4} M. The metal ion concentrations applied were calculated based on the theoretical peptide loading of the resins and the mass-increase during synthesis, according to

$$L = \frac{L_{\mathrm{i}}}{1.0 + L_{\mathrm{i}} \times M_{\mathrm{ad}}}$$

where L stands for the loading of the resin after synthesis, L_{i} denotes the original loading value and M_{ad} is the molar mass of the added peptide fragment. Based on these calculations, the loadings of YY-BHA and YY-NTG are 0.497×10^{-3} and 0.218×10^{-3} mole·g^{-1}, respectively. The applied $CdCl_2$ concentrations for a specific experiment were calculated by considering the amount of one equivalent of Cd(II) that could bind to each immobilized ligand. In this approach, the theoretical Cd(II)-binding capacity of YY-BHA and YY-NTG should be 0.497×10^{-3} mole g^{-1} (= 55.9 mg/g) and 0.218×10^{-3} mole g^{-1} (= 24.5 mg/g), respectively. Relative to this quantity, the 10.0 mL $CdCl_2$ samples contained ca. 33, 66, 100, 150, 200 or 300 % Cd(II), depending on the type of experiment to be performed. The resin batches were contacted with the $CdCl_2$ solutions for 60 min with vertical rotational shaking that was followed by centrifugation (10 min, 4000 rpm) assuring the settling of resin beads. 1 mL liquid aliquots were taken from each samples and diluted to 100 mL before determining the residual Cd concentration by ICP-MS. In the experiments involving the hexapeptide immobilized on silica plate supports (YY-G and YY-Q), the same approach as above was employed, taking also into account the significantly lower capacity (surface ligand density) of these samples. All of the data presented below is the result of triplicate experiments except the

Cd(II) binding capacity data for YY-NTG, which was determined by experiments carried out in five repetitions.

For the metal ion selectivity experiments, a solution containing the mixture of Cd(II), Zn(II) Ni(II) and Pb(II) ions, as their nitrates, was added to the immobilized peptide so that the final concentrations of each metal ions in a 10.0 mL sample were ca. 50 or 100 % relative to the theoretical loading of YY-NTG, i.e. 1.15×10^{-3} M or 2.30×10^{-3} M.

Results and discussion

The hexapeptide probe

The studied oligopeptide was designed after one of nature's well-known metal ion capturing short amino acid sequence, Cys-X-X-Cys, characteristic to the metal binding domains of a variety of metalloproteins like methallothioneins of various types [45,46] or several metal sequestering and transport proteins including e.g. the bacterial MerP,[47] the P1-type heavy metal transporting ATPases ZntA and CadA from bacteria [48] or the human ATP7A and ATP7B.[49] The fluorophore tyrosine residues were introduced as potential transducing elements for future application of the ligand as a metal ion receptor in optochemical sensors. The two internal polar serine units allow for a good accessibility of the peptide chain by water molecules. Peptides containing the Cys-X-X-Cys fragment were shown in the literature to form remarkably stable complexes with various soft/borderline metal ions, including Zn(II) or Cd(II) [50,51] and Hg(II) [50,52] owing to the high affinity of the Cys thiolates towards these ions. Indeed, Cys-thiolate was shown to be the primary anchor for Cd(II) also in cases when other potential donor groups were present.[53] Serine and tyrosine sidechains have been proposed to

have only a weak effect, if any, on the stability of Cd(II)-peptide complexes [54] and thus Ser and Tyr residues in the presently studied ligand are not supposed to play a significant role in the binding of Cd(II). It is also worth noting that Cd(II)-induced amide nitrogen deprotonation and coordination has been ruled out in case of any previously studied cysteine containing peptides.[54]

Investigation of the Cd(II)-binding features of the designed hexapeptide in aqueous solution was meant to provide valuable information in advance of studies on the solid supported systems. However, the observed poor solubility of the ligand allowed only the testing of the effect of Cd(II)-binding on the fluorescence intensity attributed to the tyrosine fluorophores. The stepwise addition of the metal ion to the solution of YY resulted in a fluorescence quenching up to ca. a 1:1 Cd(II) to YY ratio above which no further notable decrease of intensity appeared (Figure 3). The shape of the depicted trace of fluorescence spectra (λ = 308 nm) and the remarkable drop of intensity already at a 0.5:1 metal ion to ligand ratio suggest that the observed quenching of fluorescence is not due to a single bound species. Nevertheless, the experiment proves that the tested Tyr-containing molecular probe can indeed signal the binding of the metal ion via fluorescence transduction, thus potentially can be used in an optochemical construction.

The designed hexapeptide was immobilized, in other words synthesized directly, on the surface of solid supports (resin beads and silica plates), according to the procedures described in chapters “Peptide synthesis on synthetic resins” and “Peptide synthesis on silica surfaces”.

Study of the cadmium(II) binding properties

Cd(II)-binding properties of YY-BHA and YY-NTG were studied under various starting conditions and the latter one was compared to the ability of the capped-NTG (a reference containing no peptide) in capturing metal ions from liquid samples. For the capped-NTG, no decrease of the Cd(II) concentration at any pH was observed after contacting with $CdCl_2$ solutions for 60 min.

The two resin supports showed fundamentally different behavior in terms of the metal ion capturing properties of the peptide immobilized on their surface. While YY-NTG appeared to have a remarkable Cd(II)-coordination ability, practically no Cd(II) ion binding was observed for YY-BHA. Most probably this difference can be attributed to the different swelling of the resins; the PEG-based NTG resin swells significantly better. Accordingly, detailed studies were only performed with the YY-NTG, as detailed below. For practical reasons, these detailed studies were not carried out with YY-G and YY-Q, only the capacity measurements, as described later.

Effect of contact time

Studies were also carried out to determine the optimal contact time needed to complete the Cd(II)-binding by the immobilized peptides. Batches of YY-NTG (m = 10.0 mg each) were contacted with 10.0 mL of $CdCl_2$ solution adjusted to pH = 7.0, containing a ca. 1.5-fold excess of Cd(II) over the immobilized ligand, for various times (durations of 15, 30, 60, 120, 180 min were tested). It was found that after as short as only 15 min, the level of Cd(II) binding reached ca. 80% of the final (saturation) capacity. The Cd(II) binding level remained the same, within experimental error, for contact times over 30 min. However, in order to ensure a complete equilibration, a 60 min reaction time was applied in later experiments monitoring the effect of pH and Cd(II) concentration.

Effect of pH

The effect of pH on the Cd(II)-binding of YY-NTG was monitored in samples containing a ca. 1.5-fold excess of metal ion relative to the quantity of immobilized ligand present in 10.0 mg of YY-NTG. As seen on the bound Cd(II) vs. pH graph (Figure 4), practically no metal ion binding occurs at pH 2. The increase of pH results in a notable increase of the Cd(II)-capturing ability which levels off around pH ~ 4–5. The observed Cd(II)-binding capacity (ca. 0.12 mg /10 mg) is about 49% of the nominal value (0.245 mg/10 mg) which would refer to the situation that all binding site of the resin was fully loaded with the ligand and each YY peptide would bind one equivalent of Cd(II). Experiments at higher pH (pH = 8.0 and 9.0) were also conducted, however, the formation of white flaky precipitate was observed, most likely indicating the hydrolysis of Cd(II).

Effect of metal ion concentration

The influence of the total concentration of Cd(II) at pH = 7.0 was monitored in a series of experiments where the Cd(II):peptide ratio was varied between 1:3 and 3:1. The obtained profile (Figure 5) shows a monotone increase with a saturation shape leveling at a value of ca. 0.135 mg Cd(II)/10.0 mg YY-NTG. Again, this binding capacity is about 50% smaller than the nominal value. It has to be kept in mind, however, that there can be unreacted linkage sites in the resin that would mean a smaller theoretical capacity as compared to the nominal 0.245 mg/10 mg. Besides, the homogeneity of YY-NTG may not be perfect which can result in a certain level of fluctuation of the observed metal ion binding capacity, as is discussed in the "Assessment of the analytical features of the probe" section. Nevertheless, the presented results clearly show that YY-NTG is capable of the efficient capturing of Cd(II) under the applied conditions.

Equilibrium studies

In order to further elucidate the Cd(II)-binding properties of YY-NTG, pH-potentiometric titrations were performed in aqueous samples between pH 2 – 11, containing a known, weighed amount of YY-NTG beads (ca. 30.0 mg) in the absence and presence of Cd(II) ions.

Titration curves of the resin without Cd(II) reflect overlapping deprotonation processes taking place in the basic pH-range (Figure 6). Data could be well fitted by considering four consecutive deprotonation steps corresponding to dissociation of the two cysteine sidechain thiol and two tyrosine sidechain phenol groups. The determined pK_a values (shown in Table 1) fall in the range characteristic to Cys [33,51] and Tyr residues [55,56] within a peptide chain.

In the presence of Cd(II), the overall shape of the curves are similar, for the first look, to that of the metal ion free solution. However, ca. 1.5 and 2 equivalents per ligand extra base consumption occurs up to pH ~ 7 in the samples containing Cd(II) and YY-NTG in a 0.5:1 and ~1:1 ratio, respectively (see Figure 6). Please note that the latter titration, as a precaution, was carried out using a small (10 %) YY-NTG excess for preventing a possible hydrolysis of Cd(II) ions. According to the well-known strong affinity of Cd(II) towards the soft sulfur donors of the Cys-thiolate group, the observed base consumption below pH 7 is the result of Cd(II)-induced Cys-deprotonation and metal ion binding to these residues taking place already at a relatively low pH. This observation is fully coherent with literature data published on the interaction of Cd(II) with short Cys-containing peptides.[51,53,57] In the equimolar system of Cd(II) and YY-NTG, the coordination of both Cys residues is obvious, based on the titration data, whereas the deprotonation of the Tyr-side chains are only slightly affected, and these groups very likely do not participate in Cd(II)-binding. Since more than one base equivalent is consumed up to neutral pH in the Cd(II):YY-NTG 0.5:1 system, the binding of

more than two cysteines to Cd(II) can be proposed. It means that besides/instead of 1:1 species, bis-ligand type structures, in which two immobilized YY are bound to one Cd(II), also have to be present. The best model obtained in the evaluation of the potentiometric results are given in Table 1 representing also the overall stabilities of the Cd(II)-YY-NTG associates (see the Experimental for the definitions).

The species distribution diagrams (Figure 7), calculated for the conditions of the metal ion capturing studies (and for the potentiometric studies in the Supporting Information, Figure S2.A-B), show that the formation of metal ion complexes starts slightly below pH 3 and the majority of Cd(II) is bound to the ligand already at pH ~ 5. CdH_2L, with two coordinated Cys-thiolates is a major species in a broad pH-range. However, a bis-complex, CdH_5L_2, becomes dominant when the immobilized peptide is in an excess over the added Cd(II) (see the solid lines on Figure 7 (and Figure S2.B)). A probable reason for the relatively high stability of this bis-complex lies in the immobilized nature of the ligands (close vicinity of available donor groups) and thus the binding of a second molecule may be favored when sub-equivalent Cd(II) concentration is present. The deprotonation process leading to CdH_4L_2 is presumably a proton release from the second Cys residue, nevertheless CdHL and CdH_3L_2 are likely to be formed by the deprotonation of Tyr-phenol side chains (taking place only above pH ~ 9, see data in Table 1 and the species distribution diagrams, Figure S2.A-B, in the Supporting Information). The apparent stability constant ($K_{app} = 1.3\times10^{10}$) calculated for pH = 7.0 at a 1:1 Cd(II):YY-NTG ratio based on the equation

$$K_{app} = \frac{\Sigma[Cd^{2+}]_{bound}}{[Cd^{2+}]_{free} \times \Sigma[YY\text{-}NTG]_{free}}$$

is more than 70 times higher compared to the calculated stability of a 12-mer peptide containing other coordinating donor groups (His and Asp) besides two cysteines [33] and ca. 8 – 140 times higher than the stabilities that can be calculated for a other relatively short peptides

where Cd(II) was shown to be coordinated by the two cysteine residues of the ligands.[50,51,57] A column chart demonstrating the apparent stabilities for the Cd(II)-binding of these ligands at pH 7.0 as compared to that of YY-NTG is included in the Supporting Information (Figure S3). This stability difference, in favor of YY-NTG, may originate partly from the immobilized, more rigid nature of the studied YY ligand, i.e. less entropy is lost upon metal ion binding as compared to the metal ion binding process of the peptides studied in solution phase. Stability data for the Cd(II)-binding of immobilized cysteine containing peptides are very scarce in the literature and even the available results are difficult to compare to YY-NTG due to e.g. the polymeric nature/behavior of the surface-linked systems (see below) or to the different applied conditions (i.e. pH, temperature). Polycysteine and cysteine, when coupled to a porous carbon surface, were shown to possess several type of binding sites displaying variable binding affinities, as determined by breakthrough experiments.[35] In contrast, cysteine immobilized onto poly(hydroxyethylmethacrylate) microbeads or monoliths was found to capture one Cd(II) ion per amino acid units and the determined stabilities were K_{app} = 4.35×10^4 and 5.28×10^4 M^{-1}, respectively.[58,59]

In summary, the determined K_{app} value for the system definitely reflects a remarkable binding affinity of the YY hexapeptide towards Cd(II).

The distribution of the immobilized YY between the non-bound (H_4L) and the various Cd(II)-bound forms is in a good coherence with the binding capacity determined by the metal ion capturing studies with ICP-MS. According to Figure 7, a significant fraction of YY is in a non-bound state at pH ~ 3.8, the pH observed at the end of the Cd(II)-binding experiments. Indeed, ca. 60 and 40% of YY is in its fully protonated H_4L form when the Cd(II):YY-NTG ratio is 0.66:1 (Figure 7 solid lines) and 1.5:1 (Figure 7 dashed lines), respectively. This is exactly what the bound Cd(II) vs. $c_{Cd(II)}$ and the bound Cd(II) vs. pH profiles imply (Figure 5 and Figure 6, respectively). On the other hand, in the presence of Cd(II)-excess, the

immobilized ligands should be fully loaded by Cd(II) which is proved by the metal ion binding experiment performed under controlled pH (see in a later chapter).

The pH-potentiometric results reflect a Cd(II)-concentration dependent equilibrium between various Cd(II)-YY-NTG species in the whole studied pH-range. Due to this, the strong Cd(II)-binding affinity of the hexapeptide ligand can be utilized for analytical purposes in a future construct only under controlled pH and with the support of a multipoint calibration covering the complete applicable concentration range of the probe.

Assessment of the analytical features of the probe

In view of potential sensor applications, some analytical features of the molecular probe were also tested. For practical reasons, already outlined earlier, most of these tests were carried out with YY-NTG samples, but some were also conducted on YY-G or YY-Q.

Capacity

As was alluded to above, YY-BHA was not capable of capturing Cd(II) neither at acidic nor at neutral pH. This is presumably due to the hydrophobic bead material that causes a very poor swelling of the resin in aqueous matrices which may lead to the inaccessibility of the covalently attached YY peptides by the metal ions from the solution phase. On the other hand, YY-NTG was proved to have a remarkable potential in the capturing of Cd(II). The Cd(II) capacity of YY-NTG was determined from 5 parallel experiments using a 4.08×10^{-4} M $CdCl_2$ solution with a pH adjusted to ~6.0 (to minimize the risk of metal ion hydrolysis) before adding the 10.0 mg batches of YY-NTG into 10.0 mL of the metal ion solution. The capacity measured this way is 11.5 mg/g with a repeatability of 10% RSD.

We also measured the capacity of YY-Q samples, using 10 mL of a 100 μg/L Cd solution set to pH= 7.0 with HEPES buffer. It was found that each YY-Q plate bound an average of 0.225 μg Cd(II), which is 64.1% of the estimated capacity (0.351 μg/plate). This finding indicates a good efficiency of the synthesis (immobilization) and of the Cd(II) binding also on silica supports.

It is worth mentioning that the above capacity values were found to be further improvable by pH buffering, as can be read in the following chapter. Furthermore, data in Figures 3 and 5 suggests that at least one order of magnitude dynamic range can be achieved using this molecular probe and a multipoint calibration curve.

Effect of pH buffering

The pH of each sample was also monitored after a reaction with the resin beads had been completed. It was observed that the pH of the solutions, initially adjusted to pH = 5.0 or above before the Cd(II) loading, shifted towards a more acidic pH during the experiments. In fact, the post-loading pH values were found to be around 3.8 independently from the starting pH value. This effect is caused by the release of protons from the ligands as a result of metal ion coordination. By glancing at Figure 4, it can be realized that this acidic pH shift towards values of about pH=4 results in a significant loss in cadmium(II) binding capacity. Similar pH-dependence was observed previously in the Cd^{2+}, Cu^{2+} and Zn^{2+} binding efficiency of EDTA immobilized on a silica support, which was explained by the availability of a decreasing fraction of ionized donor groups caused by the decrease of the pH[60] In order to test the capacity of YY-NTG under strictly controlled pH, we prepared a sample containing a 1.5-fold excess of metal ion relative to the quantity of immobilized ligand as well as HEPES buffer (c = 0.02 M) with the pH adjusted to 7.0. After the usual 60 min equilibration, we managed to come near the nominal capacity of YY-NTG (assuming that one Cd(II) per

immobilized ligand is captured). The determined metal ion binding capacity of YY-NTG under these conditions was found to be 0.243 mg/10.0 mg. These findings efficiently illustrate the necessity of pH buffering in an analytical application of the YY probe. We would also like to point out to that the near-neutral pH of most natural water samples (pH= 6-7.5) is in fact ideal for the studied probe (highest capacity).

Probe regeneration and ageing

We have also tested whether the used YY-NTG samples could be regenerated, as this is an important feature of a molecular probe meant for sensor applications. For this purpose, an efficient polydentate metal ion chelator, EDTA, was utilized after an acidic treatment of the molecular probe. Based on the formation constant of the Cd(EDTA) complex ($\log\beta$ = 16.50 [61]) and the acid dissociation constants of EDTA [61] one can calculate an apparent stability constant for the same conditions used in the calculations for YY-NTG (see in "Equilibrium studies"). The K_{app} value for the Cd(II) – EDTA system at pH = 7.0 is 1.2×10^{13}, which is almost three orders of magnitude larger than the apparent stability constant for Cd(II) – YY-NTG (see before). This data supports the expectation that EDTA can be efficiently used for removing Cd(II) from the probe.

The collected, formerly Cd(II)-loaded YY-NTG resin beads were washed with deionized water, treated with a 0.01 M HCl solution, washed again and then soaked in a 0.02 M EDTA solution for 30 min. Finally, the resin beads were washed again, rinsed with methanol and dried overnight under vacuum. Repeated Cd(II)-binding experiments with the previously used YY-NTG showed a full recovery (105.4 %) of metal ion binding.

The capacity of YY-NTG was observed to slightly decrease over time (ageing). A ca. 20 % capacity loss was observed after several months of keeping the resin under argon atmosphere at t = 4 °C. The capacity loss was found to be fully recoverable by the addition of

dithiothreitol (c = 0.01 M solution), a reduction agent, and stirring for 60 min. This finding proves that the ageing effect is due to the slow oxidation of the cysteine moieties of the peptide caused by oxygen traces.

Metal ion selectivity

We also briefly studied the selectivity of the YY-NTG hexapeptide probe for a few selected metal ions. In this test, the metal ion binding experiments were performed by applying solutions that contained Cd(II), Zn(II), Ni(II) and Pb(II) ions in a 1:1:1:1 ratio with total concentrations representing ca. two- and four-fold metal ion excess relative to the theoretical capacity of YY-NTG. The bound amounts of Zn(II), Ni(II) and Pb(II) ions were found to be 15%, 55% and 90%, respectively, relative to the bound amount of Cd(II) (100 %). This trend is in accordance with the literature data for the order of the affinities of these metal ions towards 2-Cys containing peptides or other dithiol compounds.[33,34,51,62,63]

Conclusions

The novel hexapeptide Ac-YCSSCY–, either immobilized on the surface of a hydrophilic resin (YY-NTG), or glass or quartz surfaces (YY-G and YY-Q), showed a remarkable efficiency in the binding of Cd(II). The capturing of Cd(II) is pH-dependent with an optimum around neutral pH. As proved by equilibrium studies each immobilized peptide can bind one Cd(II) ion in the presence of one equivalent or more metal ion. Under metal deficient conditions, two peptides may also coordinate to the captured Cd(II) ions suggesting that a potential sensor application of the studied molecular probe would require a multipoint calibration and a controlled pH for metal ion sensing. The resin supported probe can be easily

regenerated by applying a metal ion chelator, such as EDTA. It was also successfully demonstrated that the developed molecular probe provides a sensitive fluorescence signal (quenching) as a function of Cd(II) concentration. Assuming a practical 10 mL volume for the sample solution and a YY receptor coverage on a silica fiber optic chemical sensor active surface, similar to the coverage determined in our experiments for quartz substrates (YY-Q), it is estimated that this molecular probe can be used for the measurement of Cd(II) around and below 22.5 μg/L (200 nM) concentration. This value is well within the range of the LOD values published in the literature for other fluorescent Cd(II)-sensing peptidyl probes.[18,32]

Variants of the studied short peptide sequence, in which one of the Tyr residues is substituted with an Asp unit and thereby have considerably better solubility in water and therefore allow more detailed equilibrium studies in the liquid phase, can also be synthesized. At present, this synthesis and extensive characterization work is underway in our laboratory.

Acknowledgments

The authors acknowledge the financial support received from the European Union's European Regional Development Fund, provided within the frameworks of the Hungary-Romania Cross-Border Cooperation Programme 2007-2013 under project No. HURO/1001/232/2.2.2. (METCAP). AJ wishes to thank the financial support of the János Bolyai Research Grant from the Hungarian Academy of Sciences. CM acknowledges the financial support of the strategic grant POSDRU/159/1.5/S/137070 (2014) of the Ministry of National Education, Romania, co-financed by the European Social Fund-Investing in People, within the Sectorial Operational Programme Human Resources Development 2007-2013. The

authors are indebted to Judit Kopniczki (University of Szeged, Department of Optics and Quantum Electronics) for her kind assistance in the AFM and SEM experiments.

References

1 S. C. Warren-Smith, S. Heng, H. Ebendorff-Heidepriem, A. D. Abell, T. M. Monro, *Langmuir* **2011**, *27*, 5680.

2 N. W. Hayes, C. J. Tremlett, P. J. Melfi, J. D. Sessler, A. M. Shaw, *Analyst* **2008**, *133*, 616.

3 H. Guillemain, M. Rajarajan, T. Sun, K. T. V Grattan, *Meas. Sci. Technol.* **2009**, *20*, 045207.

4 L. Malachowski, J. L. Stair, J. A. Holcombe, *Pure Appl. Chem.* **2004**, *76*, 777.

5 B. Imperiali, D. A. Pearce, J.-E. Sohna Sohna, G. Walkup, A. Torrado, *SPIE Proc.*, ed. by M. Fallahi, B. I. Swanson, Boston, MA, **1999**, pp. 135–143.

6 L. Prodi, *Coord. Chem. Rev.* **2000**, *205*, 59.

7 N. Verma, M. Singh, *BioMetals* **2005**, *18*, 121.

8 Q. Liu, J. Wang, B. J. Boyd, *Talanta* **2015**, *136*, 114.

9 I. Bontidean, J. R. Lloyd, J. L. Hobman, J. R. Wilson, E. Csöregi, B. Mattiasson, N. L. Brown, *J. Inorg. Biochem.* **2000**, *79*, 225.

10 A. Torrado, G. K. Walkup, B. Imperiali, *J. Am. Chem. Soc.* **1998**, *120*, 609.

11 L. N. Neupane, P. Thirupathi, S. Jang, M. J. Jang, J. H. Kim, K.-H. Lee, *Talanta* **2011**, *85*, 1566.

12 J.-M. Kim, C. R. Lohani, L. N. Neupane, Y. Choi, K.-H. Lee, *Chem. Commun. (Camb).* **2012**, *48*, 3012.

13 B. P. Joshi, C. R. Lohani, K.-H. Lee, *Org. Biomol. Chem.* **2010**, *8*, 3220.

14 P. Wang, L. Liu, P. Zhou, W. Wu, J. Wu, W. Liu, Y. Tang, *Biosens. Bioelectron.* **2015**, *72*, 80.

15 H. A. Godwin, J. M. Berg, *J. Am. Chem. Soc.* **1996**, *118*, 6514.

16 B. R. White, H. M. Liljestrand, J. A. Holcombe, *Analyst* **2008**, *133*, 65.

17 G. K. Walkup, B. Imperiali, *J. Am. Chem. Soc.* **1997**, *119*, 3443.

18 B. P. Joshi, J. Park, W. I. Lee, K.-H. Lee, *Talanta* **2009**, *78*, 903.

19 T. Kochańczyk, P. Jakimowicz, A. Krężel, *Chem. Commun. (Camb).* **2013**, *49*, 1312.

20 B. P. Joshi, W.-M. Cho, J. Kim, J. Yoon, K.-H. Lee, *Bioorg. Med. Chem. Lett.* **2007**, *17*, 6425.

21 B. P. Joshi, K.-H. Lee, *Bioorg. Med. Chem.* **2008**, *16*, 8501.

22 B. P. Joshi, J.-Y. Park, K.-H. Lee, *Sensors Actuators B Chem.* **2014**, *191*, 122.

23 M. Dutta, D. Das, *TrAC Trends Anal. Chem.* **2012**, *32*, 113.

24 L. Prodi, M. Montalti, N. Zaccheroni, J. S. Bradshaw, R. M. Izatt, P. B. Savage, *Tetrahedron Lett.* **2001**, *42*, 2941.

25 R. T. Bronson, D. J. Michaelis, R. D. Lamb, G. A. Husseini, P. B. Farnsworth, M. R. Linford, R. M. Izatt, J. S. Bradshaw, P. B. Savage, *Org. Lett.* **2005**, *7*, 1105.

26 M. Choi, M. Kim, K. D. Lee, K.-N. Han, I.-A. Yoon, H.-J. Chung, J. Yoon, *Org. Lett.* **2001**, *3*, 3455.

27 T. Gunnlaugsson, T. Clive Lee, R. Parkesh, *Tetrahedron* **2004**, *60*, 11239.

28 G. M. Cockrell, G. Zhang, D. G. VanDerveer, R. P. Thummel, R. D. Hancock, *J. Am. Chem. Soc.* **2008**, *130*, 1420.

29 Y. Zhou, Y. Xiao, X. Qian, *Tetrahedron Lett.* **2008**, *49*, 3380.

30 Y. Yang, T. Cheng, W. Zhu, Y. Xu, X. Qian, *Org. Lett.* **2011**, *13*, 264.

31 J. M. Kim, B. P. Joshi, K. H. Lee, *Bull. Korean Chem. Soc.* **2010**, *31*, 2537.

32 Y. Li, L. Li, X. Pu, G. Ma, E. Wang, J. Kong, Z. Liu, Y. Liu, *Bioorg. Med. Chem. Lett.* **2012**, *22*, 4014.

33 A. Jancsó, D. Szunyogh, F. H. Larsen, P. W. Thulstrup, N. J. Christensen, B. Gyurcsik, L. Hemmingsen, *Metallomics* **2011**, *3*, 1331.

34 A. Jancsó, B. Gyurcsik, E. Mesterházy, R. Berkecz, *J. Inorg. Biochem.* **2013**, *126*, 96.

35 T. C. Miller, J. A. Holcombe, *Anal. Chim. Acta* **2002**, *455*, 233.

36 H. A. Jurbergs, J. A. Holcombe, *Anal. Chem.* **1997**, *69*, 1893.

37 E. Gutierrez, T. C. Miller, J. R. Gonzalez-Redondo, J. A. Holcombe, *Environ. Sci. Technol.* **1999**, *33*, 1664.

38 E. Kaiser, R. L. Colescott, C. D. Bossinger, P. I. Cook, *Anal Biochem* **1970**, *34*, 595.

39 A. Carré, W. Birch, V. Lacarriere, *Silanes Other Coupling Agents, Vol. 4*, ed. by K. L. Mittal, CRC Press, Boca Raton, FL, USA, **2007**, pp. 113–126.

40 M. Phaner-Goutorbe, V. Dugas, Y. Chevolot, E. Souteyrand, *Mater. Sci. Eng. C* **2011**, *31*, 384.

41 L. Malachowski, J. Stair, *Pure Appl. Chem.* **2004**, *76*, 777.

42 E. Metwalli, D. Haines, O. Becker, S. Conzone, C. G. Pantano, *J. Colloid Interface Sci.* **2006**, *298*, 825.

43 J. R. Lakowicz, *Principles of Fluorescence Spectroscopy*, 3rd ed., Springer US, New York, **2006**.

44 L. Zékány, I. Nagypál, G. Peintler, *PSEQUAD for Chemical Equilibria*, Technical Software Distributors, Baltimore, MD, **1991**.

45 N. Romero-Isart, M. Vašák, *J. Inorg. Biochem.* **2002**, *88*, 388.

46 C. Blindauer, *J. Biol. Inorg. Chem.* **2011**, *16*, 1011.

47 S. J. Opella, T. M. DeSilva, G. Veglia, *Curr. Opin. Chem. Biol.* **2002**, *6*, 217.

48 L. Banci, I. Bertini, S. Ciofi-Baffoni, X.-C. Su, R. Miras, N. Bal, E. Mintz, P. Catty, J. E. Shokes, R. A. Scott, *J. Mol. Biol.* **2006**, *356*, 638.

49 J. R. Forbes, G. Hsi, D. W. Cox, *J. Biol. Chem.* **1999**, *274*, 12408.

50 P. Rousselot-Pailley, O. Sénèque, C. Lebrun, S. Crouzy, D. Boturyn, P. Dumy, M. Ferrand, P. Delangle, *Inorg. Chem.* **2006**, *45*, 5510.

51 K. Krzywoszynska, M. Rowinska-Zyrek, D. Witkowska, S. Potocki, M. Luczkowski, H. Kozlowski, *Dalton Trans.* **2011**, *40*, 10434.

52 S. Pires, J. Habjanič, M. Sezer, C. M. Soares, L. Hemmingsen, O. Iranzo, *Inorg. Chem.* **2012**, *51*, 11339.

53 V. Dorcak, A. Krezel, *Dalton Trans.* **2003**, 2253.

54 I. Sóvágó, K. Várnagy, *Met. Ions Life Sci.* **2013**, *11*, 275.

55 W. Bal, M. Jezowska-Bojczuk, H. Kozlowski, L. Chruscinski, G. Kupryszewski, B. Witczuk, *J. Inorg. Biochem.* **1995**, *57*, 235.

56 M. Rowinska-Zyrek, S. Potocki, D. Witkowska, D. Valensin, H. Kozlowski, *Dalton Trans.* **2013**, *42*, 6012.

57 K. Kulon, D. Woźniak, K. Wegner, Z. Grzonka, H. Kozłowski, *J. Inorg. Biochem.* **2007**, *101*, 1699.

58 A. Dişbudak, S. Bektaş, S. Patır, Ö. Genç, A. Denizli, *Sep. Purif. Technol.* **2002**, *26*, 273.

59 L. Uzun, D. Türkmen, E. Yılmaz, S. Bektaş, A. Denizli, *Colloids Surfaces A Physicochem. Eng. Asp.* **2008**, *330*, 161.

60 D. Q. Melo, V. O. S. Neto, J. T. Oliveira, A. L. Barros, E. C. C. Gomes, G. S. C. Raulino, E. Longuinotti, R. F. Nascimento, *J. Chem. Eng. Data* **2013**, *58*, 798.

61 A. E. Martell, R. M. Smith, R. J. Motekaitis, *NIST Critically Selected Stability Constants of Metal Complexes Database, NIST Standard Reference Database 46*, National Institute of Standards and Technology, Gaithersburg, MD, **2001**.

62 M. Rowinska-Zyrek, D. Witkowska, S. Bielinska, W. Kamysz, H. Kozlowski, *Dalton Trans.* **2011**, *40*, 5604.

63 A. Krężel, W. Leśniak, M. Jeżowska-Bojczuk, P. Młynarz, J. Brasuñ, H. Kozłowski, W. Bal, *J. Inorg. Biochem.* **2001**, *84*, 77.

Figure legends

Figure 1. AFM scans taken from the surface of a glass slide before (left panel) and after silanization (right panel). Silanized regions are identified as protruding, small, light coloured spots in the right hand side image.

Figure 2. Optical absorption spectrum of untreated and silanized glass surfaces in the nanoparticle adsorption test. The electrostatically attached gold nanoparticles cause a small, but reproducible light absorption around 600 nm.

Figure 3. Change of the fluorescence intensity of YY at λ = 308 nm as a function of the Cd(II) : YY ratio at pH = 7.0. The insert shows fluorescence spectra in the absence (dashed line) and presence (continuous line) of one equivalent of Cd(II). The presented data represent the results of two parallel experiments. (t = 25 °C, λ_{ex} = 278 nm, c_{YY} = 10.0 μM)

Figure 4. Cd(II)-binding ability of YY-NTG as a function of pH of the liquid samples that were in contact with 10.0 mg of the resin for 60 min (t = 25 °C). The data points plotted are averages based on triplicate measurements.

Figure 5. Cd(II)-binding ability of YY-NTG as a function of the Cd(II)-content of the liquid samples that were in contact with 10.0 mg of the resin for 60 min (pH = 7.0, t = 25 °C). The data points plotted are averages based on triplicate measurements.

Figure 6. Experimental and fitted (solid lines) titration data of YY-NTG in the absence (●) and presence of metal ions. Titration curves are shown as a function of base consumption normalized for the quantity of the immobilized ligand present in the samples. Please note that

the amount of base consumed by the added strong acid has been eliminated in the normalized curves. ($m_{\text{YY-NTG}}$ = 30.0 mg, $n_{\mathbf{Cd(II)}} : n_{\mathbf{YY}}$ = 0.5 : 1 (▲) and $n_{\mathbf{Cd(II)}} : n_{\mathbf{YY}}$ = 1.0 : 1 (□)).

Figure 7. The fraction of the immobilized YY in various Cd(II)-bound forms as represented by distribution diagrams calculated for two different conditions used in Cd(II)-capturing studies. Solid lines: Cd(II) : YY = 0.66 : 1, $c_{\mathbf{Cd(II)}} = 1.44\times10^{-4}$ M ; Dashed lines: Cd(II) : YY = 1.5 : 1, $c_{\mathbf{Cd(II)}} = 3.25\times10^{-4}$ M.

Table 1 Formation constants (logβ) of the proton and cadmium(II) complexes of the immobilized YY (with the estimated errors of the last digits in parentheses) and some derived pK_a values (I = 0.1 M $NaClO_4$, T = 298 K). Charges are omitted for simplicity.

H_qL_r	lgβ		pK_a	$M_pH_qL_r$	lgβ	pK_{pqr} [a]
HL	11.5(3)	p$K_{a,4}$	11.5	CdH_2L	38.4(1)	9.6
H_2L	22.4(1)	p$K_{a,3}$	10.9	CdHL	28.8(1)	–
H_3L	32.9(1)	p$K_{a,2}$	10.5	CdH_5L_2	80.5(1)	9.9
H_4L	42.3(1)	p$K_{a,1}$	9.3	CdH_4L_2	70.6(3)	10.8
				CdH_3L_2	59.8(1)	–

[a] $pK_{pqr} = \log\beta_{pqr} - \log\beta_{p(q-1)r}$

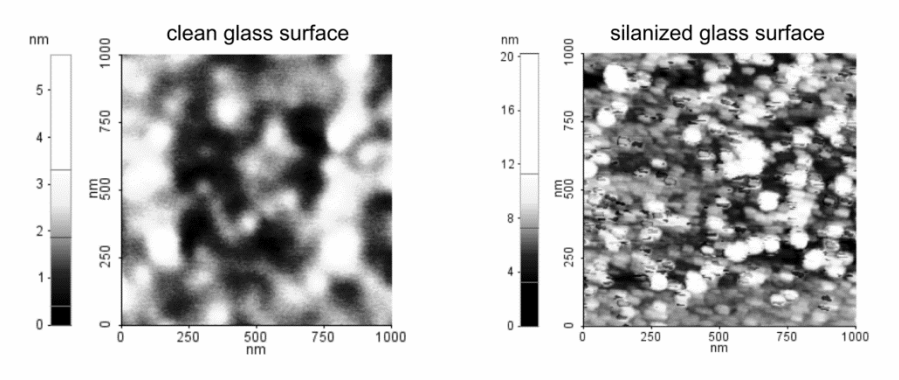

Figure 1. AFM scans taken from the surface of a glass slide before (left panel) and after silanization (right panel). Silanized regions are identified as protruding, small, light coloured spots in the right hand side image.

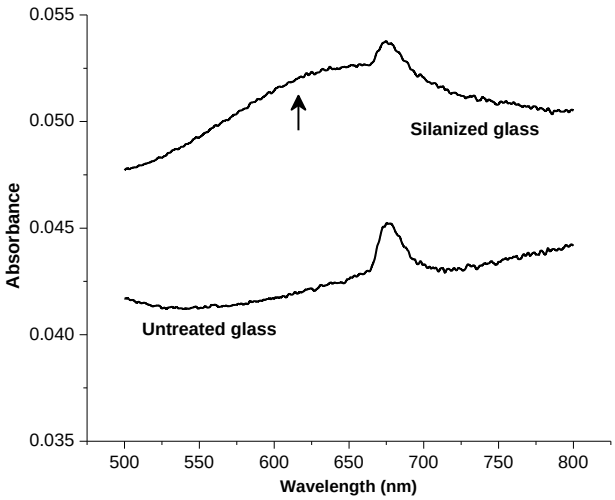

Figure 2. Optical absorption spectrum of untreated and silanized glass surfaces in the nanoparticle adsorption test. The electrostatically attached gold nanoparticles cause a small, but reproducible light absorption around 600 nm.

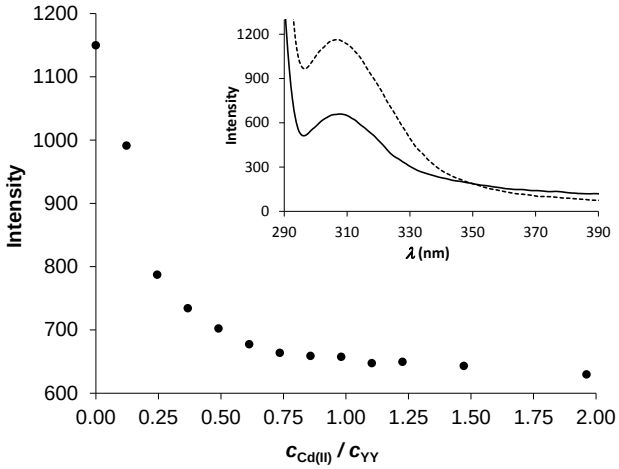

Figure 3. Change of the fluorescence intensity of YY at λ = 308 nm as a function of the Cd(II) : YY ratio at pH = 7.0. The insert shows fluorescence spectra in the absence (dashed line) and presence (continuous line) of one equivalent of Cd(II). The presented data represent the results of two parallel experiments. (t = 25 °C, λ_{ex} = 278 nm, c_{YY} = 10.0 μM)

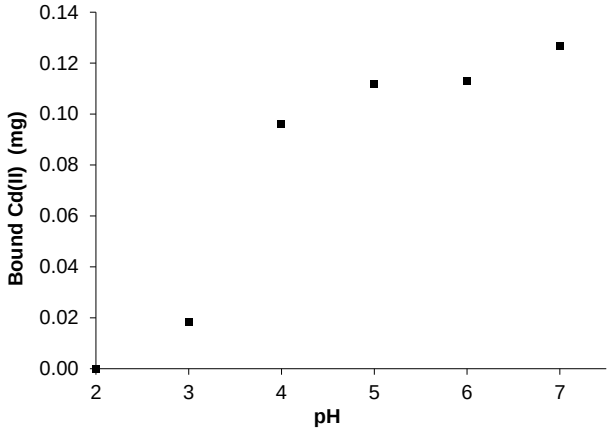

Figure 4. Cd(II)-binding ability of YY-NTG as a function of pH of the liquid samples that were in contact with 10.0 mg of the resin for 60 min (t = 25 °C). The data points plotted are averages based on triplicate measurements. Cd(II)-binding ability of YY-NTG as a function of pH of the liquid samples that were in contact with 10.0 mg of the resin for 60 min (t = 25 °C). The data points plotted are averages based on triplicate measurements.

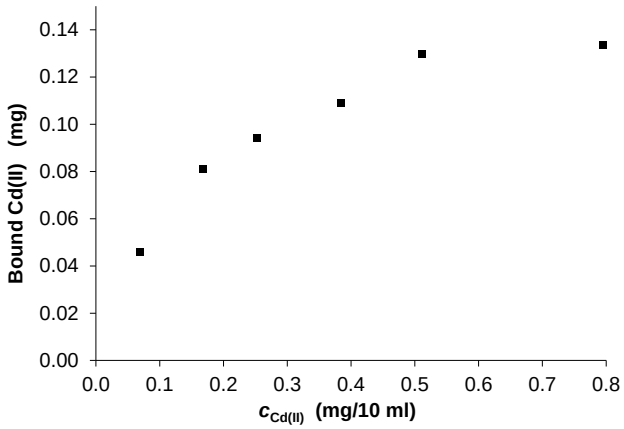

Figure 5. Cd(II)-binding ability of YY-NTG as a function of the Cd(II)-content of the liquid samples that were in contact with 10.0 mg of the resin for 60 min (pH = 7.0, *t* = 25 °C). The data points plotted are averages based on triplicate measurements.

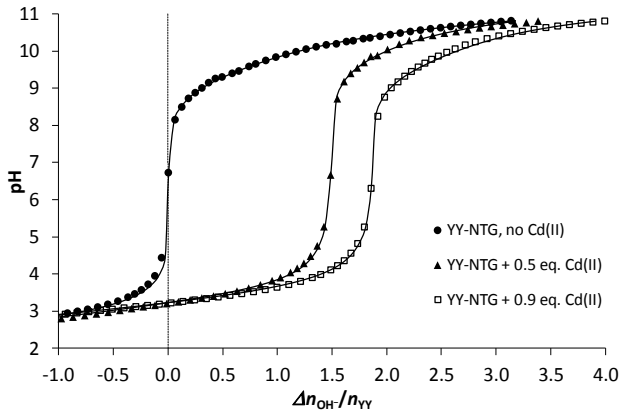

Figure 6. Experimental and fitted (solid lines) titration data of YY-NTG in the absence (●) and presence of metal ions. Titration curves are shown as a function of the base consumption normalized for the quantity of the immobilized ligand present in the samples ($m_{\text{YY-NTG}}$ = 30.0 mg, $n_{\mathbf{Cd(II)}} : n_{\mathbf{YY}}$ = 0.5 : 1 (▲) and $n_{\mathbf{Cd(II)}} : n_{\mathbf{YY}}$ = 1.0 : 1 (□)).

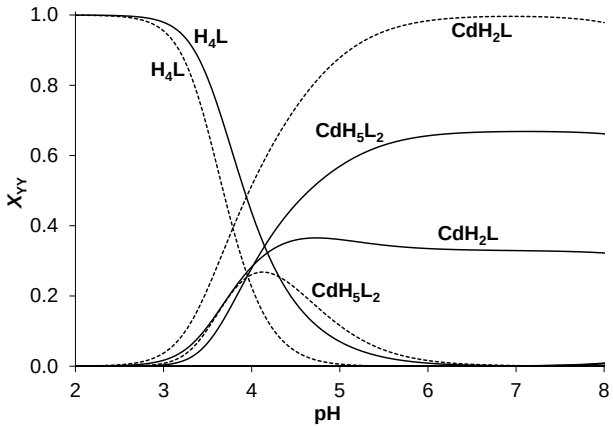

Figure 7. The fraction of the immobilized YY in various Cd(II)-bound forms as represented by distribution diagrams calculated for two different conditions used in Cd(II)-capturing studies. Solid lines: Cd(II) : YY = 0.66 : 1, $c_{\mathbf{Cd(II)}} = 1.44\times10^{-4}$ M ; Dashed lines: Cd(II) : YY = 1.5 : 1, $c_{\mathbf{Cd(II)}} = 3.25\times10^{-4}$ M.

Brief biography of the corresponding author

Prof. Attila Jancsó received his PhD in Chemistry from the University of Szeged in 2002. With the support of an EC FP5 Marie Curie Individual Fellowship he spent 2 years (2003-2004) in Prof. Harri Lönnberg's group at the University of Turku, Finland. In 2005, he joined the Bioinorganic Chemistry research group at the Department of Inorganic and Analytical Chemistry, University of Szeged. He is currently an assistant professor and his research is focused mainly on the understanding of the metal ion selectivity of metalloregulatory proteins and the design and investigation of peptide-based molecular probes for the sensing of metal ions.